Journal Pre-proof

Largely Enhanced Dielectric Properties of Polymer Composites with HfO_2 Nanoparticles for High-Temperature Film Capacitors

Lulu Ren, Lijun Yang, Siyu Zhang, He Li, Yao Zhou, Ding Ai, Zongliang Xie, Xuetong Zhao, Zongren Peng, Ruijin Liao, Qing Wang

PII: S0266-3538(20)32318-6

DOI: https://doi.org/10.1016/j.compscitech.2020.108528

Reference: CSTE 108528

To appear in: *Composites Science and Technology*

Received Date: 10 July 2020

Revised Date: 20 October 2020

Accepted Date: 25 October 2020

Please cite this article as: Ren L, Yang L, Zhang S, Li H, Zhou Y, Ai D, Xie Z, Zhao X, Peng Z, Liao R, Wang Q, Largely Enhanced Dielectric Properties of Polymer Composites with HfO_2 Nanoparticles for High-Temperature Film Capacitors, *Composites Science and Technology*, https://doi.org/10.1016/j.compscitech.2020.108528.

Author statement

L.R., X.Z. and Q.W. designed the research; L.R. and H.L. were responsible for composite preparation; L.R., L.Y., S.Z., H.L., Y.Z., D.A., Z.X., Z.P. and R.L. performed structural, dielectric and capacitive property measurements; L.R. and Q.W. wrote the manuscript with input from all authors.

Largely Enhanced Dielectric Properties of Polymer Composites with HfO_2 Nanoparticles for High-Temperature Film Capacitors

Lulu Ren,[1,2] *Lijun Yang,*[1] *Siyu Zhang,*[3] *He Li,*[2] *Yao Zhou,*[2] *Ding Ai,*[2] *Zongliang Xie,*[3] *Xuetong Zhao,*[1,*] *Zongren Peng,*[3] *Ruijin Liao*[1] *and Qing Wang*[2,*]

[1] State Key Laboratory of Power Transmission Equipment & System Security and New Technology, Chongqing University, Chongqing, 400044, China

[2] Department of Materials Science and Engineering, The Pennsylvania State University, University Park, Pennsylvania 16802, USA

[3] State Key Laboratory of Electrical Insulation and Power Equipment, Xi'an Jiaotong University, Xi'an, Shaanxi 710049, China

*Corresponding authors: X. Zhao (zxt201314@cqu.edu.cn) and Q. Wang (wang@matse.psu.edu)

ABSTRACT

Polymer dielectrics are preferred materials for high-energy-density capacitive energy storage. In particular, high-temperature dielectrics that can withstand harsh conditions, e.g., ≥150 °C, is of crucial importance for advanced electronics and electrical power systems. Herein, high-temperature dielectric polymer composites composed of polyetherimide (PEI) matrix and hafnium oxide (HfO_2) nanoparticles are presented. It is found that the incorporation of HfO_2 with a moderate dielectric constant and a wide bandgap improves the dielectric constant and simultaneously reduces the high-field leakage current density of the PEI nanocomposites. As a result, the PEI/HfO_2 composites exhibit superior energy storage performance to the current high-temperature engineering polymers at elevated temperatures. Specifically, the nanocomposite with 3 vol% HfO_2 displays a discharged energy density of 2.82 J/cm^3 at 150 °C, which is 77% higher than neat PEI. This work demonstrates the effectiveness of incorporation of the nanofiller with a medium dielectric constant into the polymer on the improvement of high-temperature capacitive properties of the polymer composites.

KEYWORDS: polymer nanocomposites, hafnium oxide nanoparticles, high temperature, dielectric properties, energy storage

1. Introduction

Polymeric materials have been widely used as dielectrics for electrostatic energy storage in electronic devices and electrical power systems. In comparison to the ceramic dielectric counterparts, polymer dielectrics feature the intrinsic advantages of light weight, long lifespan, high electric strength and graceful failure mechanism. In principle, the energy density (U_e) of dielectrics can be expressed as [1,2]

$$U_e = \int E \mathrm{d}D \tag{1}$$

where E is the applied electric field and D is the electric displacement. For linear dielectrics, the stored energy density U_e is proportional to relative permittivity (ε_r) and square of the applied electric field (E), given as [1,2]

$$U_e = \frac{1}{2}\varepsilon_0 \varepsilon_r E^2 \tag{2}$$

where ε_0 is the vacuum permittivity. The state-of-the-art capacitor film is biaxially oriented polypropylene (BOPP), which possesses frequency-independent low loss (tan $\delta \sim 1\times10^{-4}$) and high dielectric breakdown strength (~700 MV/m) [3]. These excellent properties are ascribed to the absence of polar groups in the molecular chains, which will respond to the applied electric field, generate leakage current and cause premature breakdown. On the other hand, non-polar molecular chains give rise to low dielectric constants (*e.g.* ~2.2 of BOPP), which limits the achievable energy density (*e.g.* ~2 J/cm^3 of BOPP) [1,4]. Another critical drawback of BOPP is its limited operating temperatures. Measures must be implemented either by de-rating the operating voltage or by installing passive cooling system when the operational temperature exceeds 85 °C [5].

To meet the emerging demands of energy storage under harsh conditions, the exploitation of high-temperature polymer dielectrics has attracted great interest [6,7]. High glass transition temperature (T_g) polymers such as polytetrafluoroethylene (PTFE), polycarbonate (PC), polyphenylene sulfide (PPS), polyaryletherketone (PAEK), polyimide (PI) and cross-linked divinyltetramethyldisiloxane bis(benzocyclobutene) (*c*-BCB) have been investigated in order to replace BOPP in high-temperature dielectric applications. PTFE is a class of non-polar polymer with heat resistance up to 250 ^{o}C, however, the ultralow dielectric constant (~2.0) may overshadow any other advantages gained from its low loss tangent and superior thermal stability for high-energy-density applications [8,9].Additionally, it is challenging to process PTFE into thin films by conventional approaches of melt-extrusion or solution-casting [9]. PC and PPS capacitors used to share a great market in the industry. Nevertheless, the relatively low T_gs limit their electrical properties invariance with an increasing operating temperature higher than ~125 ^{o}C [7,9,10]. For PAEK families and PI-based polymers [9,11–13], which have been commonly applied as structural materials in high-temperature aeronautical engineering. Unfortunately, their electrically insulating properties also degrades severely with the increase of temperature due to the thermally enhanced electrical conduction which is ubiquitous in the majority of polymers. *c*-BCB is a newly developed polymer which exhibits excellent properties such as ultrahigh T_g (>350 °C), low volume conductivity and low loss tangent [14,15]. However, the comparatively high-cost and not commercial-available issues limit its scalable production as of now.

As a thermoplastic engineering polymer, polyetherimide (PEI) possesses an exquisite structure in which the ether units furnish the mechanical flexibility and fluidity of

the molecular chain, and the aromatic imide units reinforce thermal resistance and mechanical strength [16,17]. Consequently, PEI exhibits the leading thermal stability, dielectric strength and reliability across a wide operating temperature window, *e.g.*, room temperature to 150 °C, compared with the abovementioned high-temperature polymers. Moreover, extensive merits such as outstanding solvent solubility, mechanical durability and flame retardancy further make PEI one of the most promising polymers for high-temperature film capacitors. Irwin *et al.* found that the PEI exerts superior insulation resistance than PC and PPS at temperatures up to 200 °C [18]. So far, PEI has been widely used as insulation components in magnet wires, electrical connectors, DC-DC converters and high-voltage switchgears [16,19]. It has also been explored for applications under extreme conditions such as aerospace and automotive industries.

Despite high dielectric strength that is critical for high energy densities, polymer dielectrics have much lower dielectric constants when compared with ceramics. In order to enhance capacitive energy densities, inorganic nanofillers with high dielectric constants have been introduced to form dielectric polymer composites [20–26]. Polymer composites consisting of ceramic fillers with high dielectric constants, *e.g.*, barium titanate ($BaTiO_3$) [27,28] and copper titanate calcium ($CaCu_3Ti_4O_{12}$), indeed exhibit improved electric displacement, but usually at the expense of much compromised breakdown strength [29,30]. For example, by adding 20 vol% $BaTiO_3$ nanoparticles into PVDF, the dielectric constant of the nanocomposite is almost doubled. In the meantime, the breakdown strength drops vastly from 325 MV/m to only 175 MV/m, which significantly limits the energy density [30]. On the other hand, the incorporation of inorganic fillers with low dielectric constants, *e.g.*, silicon dioxide (SiO_2) [5] and boron nitride nanosheet (BNNS) [12,31–34],

shows a modest impact on the dielectric constant of the composites. For instance, the incorporation of BNNSs to *c*-BCB matrix slightly improves the dielectric constant from 2.80 of pristine *c*-BCB to 3.17 of *c*-BCB nanocomposite with 14 vol% BNNSs [12]. These relatively low dielectric constant fillers contribute significantly to the large enhancements in the electric strength and the charge–discharge efficiency via reducing the high-field dielectric loss, especially at elevated temperatures [12,31,32]. While the current research efforts have mainly focused on the fillers with either high- or low- dielectric constants, much less attention has been placed on the fillers with moderate dielectric constants [35]. The study of the fillers with moderate dielectric constants with respect to polymer matrix is of great significance in order to ameliorate nanofiller induced electric field distortion and overcome the paradox between dielectric constant and dielectric strength of polymer nanocomposites.

Herein, the PEI/HfO_2 nanocomposites were prepared by a facile solution-casting method. The HfO_2 filler with a dielectric constant of ~25 and a wide bandgap of ~5.8 eV [35,36] is utilized to lessen the dielectric mismatch between the organic and inorganic phases as seen in the dielectric polymer composites with high dielectric constant fillers. It is found that the incorporation of HfO_2 nanofillers yields the improvement of the dielectric constant along with the reduction of the leakage current, which gives rise to greatly increased discharged energy densities and high charge-discharge efficiencies in the nanocomposites at various temperatures up to 150 ^{o}C.

2. Experimental Section

2.1 Sample preparation

Typically, the PEI/HfO_2 nanocomposites were fabricated by solution casting. PEI pellets (Ultem® 1000，weight average molecular weight of 54,000 and polydispersity of 2.5) were dissolved into *N*-methylpyrrolidone (NMP) (Sigma Aldrich) with the assistance of vigorous magnetic stirring at around 50 °C. By dispersing different weights of the HfO_2 nanofillers (average particle diameter of 61-80 nm, US Research Nanomaterials, Inc.) into NMP and subsequently adding PEI solution into the dispersion, the PEI/HfO_2 nanocomposite solution was obtained. The as-prepared solution underwent probe-sonication (175 W) for 30 min to achieve dispersion. The solution was cast onto a clean glass slide immediately and dried at 120 °C for 2 h and 100 °C for 17 h, respectively, to remove the solvent. Afterward, the films were peeled off from the glass substrates followed by drying in a vacuum oven at 200 °C for 24 h to further remove moisture and residual solvent. The thickness of the resultant films was controlled within 9 to 12 μm.

2.2 Characterization

The morphologies of the fracture surfaces of the polymer and composites were observed using a FEI Scios2 FIB/SEM field emission scanning electron microscope. For electrical measurements, both sides of the polymer and composite films were sputtered with gold electrodes which are 60 nm in thickness and 3 mm in diameter. Agilent HP E4980A impedance analyzer was used to measure the frequency dependence of the dielectric constant and loss tangent at room temperature (25 °C) with frequencies ranging from 10^2 to 10^6 Hz. Hewlett Packard 4140B pA meter and Trek 610D amplifier was used to acquire direct-current (DC) conduction currents under an electric field of 100 MV/m. A system in which a modified Sawyer-Tower circuit is in conjunction with a Trek Model 610E high-

voltage amplifier was used to record the high-field triangular unipolar waveform electric displacement–electric field (*D–E*) loops at frequency of 10 Hz. All the samples in *D–E* loop test were immersed into Galden HT insulation fluid to avoid discharging among air gaps. The charge-discharge tests were performed using a PK-CPR1502 test system (PolyK Technologies). The samples in were soaked in Galden HT insulation fluid and charged with applied field of 200MV/m. After charging, the charged samples was discharged to a noninductive resistor of 10.26 kΩ immediately. The thermally stimulated discharge current (TSDC) test were conducted on a system consisting of Delta Design 9023 oven, Trek 1010BHS amplifier and Hewlett Packard 4140B pA meter. The samples were firstly polarized at an electric field of 50 MV/m at a 180 °C. After 10 min, the samples were rapidly cooled to -100 °C and kept for another 10 min. The electric field was then removed and discharge current was recorded during temperature rise process, i.e. from -100 °C to 215°C at a heating rate of 3°C/min.

3. Results

Fig. 1 illustrates the cross-sectional SEM images of neat PEI and the PEI/HfO_2 nanocomposites with filler contents of 1, 5 and 9 vol%. It is found that the fillers are dispersed reasonably well in the nanocomposites even at 9 vol% filler, which afford the PEI/HfO_2 nanocomposites with excellent dielectric strength. The frequency dependence of the dielectric constant and the loss tangent of the PEI/HfO_2 nanocomposites at 25 °C is illustrated in Fig. 2a. For all the PEI/HfO_2 nanocomposites with varied filler contents, the dielectric constant is stable and exhibits almost frequency-independent features across the investigated frequency range. The loss tangents are lower than 0.005 at the frequencies ranging from 10^3 to 10^6 Hz. Fig. 2b reveals the dependence of the dielectric constant and

the loss tangent at 10^3 Hz as a function of filler content. The dielectric constant of the PEI/HfO_2 nanocomposites increases monotonically with the increase of HfO_2 content, e.g. from 3.26 of neat PEI [16] to 3.85 of the PEI/HfO_2 nanocomposites with 9 vol% filler content. This enhancement can be ascribed to the relatively higher dielectric constant (~25) of HfO_2 filler compared with PEI. Concurrently, the loss tangent increases slightly from 0.0039 to 0.0047 of the PEI/HfO_2 nanocomposites with increasing the filler content from 1 vol% to 9 vol%. The increased dielectric loss is typically related to the interface polarization between the filler and the polymer matrix phases [37–39].Note that the loss tangent of the PEI/HfO_2 nanocomposites, which is at the order of magnitude of 10^{-3}, is much lower than those of many other dielectric polymers and polymer composites, e.g., poly(methyl methacrylate) [22] and poly(vinylidene fluoride) [40].

Room temperature capacitive energy storage performance and breakdown strength of neat PEI and the PEI/HfO_2 nanocomposites was investigated by using the Sawyer-Tower circuit. The comparison of *D*–*E* loops for neat PEI and the PEI/HfO_2 nanocomposites with varied filler contents at an electric field of 300 MV/m is depicted in Fig. 3a. It is evident that the incorporation of the HfO_2 nanofillers steadily improves the electric displacement (*D*) while maintaining high charge–discharge efficiency above 95%. The maximum displacement at 300 MV/m of the PEI/HfO_2 nanocomposites increases with the increase of filler content, *i.e.*, from 9.77×10^{-3} C/m^2 of neat PEI to 1.03×10^{-2} , 1.07×10^{-2}, 1.11×10^{-2}, 1.14×10^{-2}, 1.22×10^{-2} C/m^2 of the PEI/HfO_2 nanocomposites with the filler contents of 1, 3, 5, 7 and 9 vol%, respectively. The maximum displacement shows the same trend as the dielectric constant because *D* is linearly dependent on ε_r for linear dielectrics as follow:

$$D = \varepsilon_0 \varepsilon_r E \tag{3}$$

Fig. S1a compares the charge–discharge efficiency of neat PEI and the PEI/HfO_2 nanocomposites at various electric fields. When the filler content is lower than 3 vol%, the composites have similar charge–discharge efficiencies to neat PEI, but a further increase in the filler content results in the decrease of the efficiency especially at high electric fields. It is thought that the increase of the filler content increases the particle-particle interactions, which leads to the increase in conduction loss and subsequent reduction in the efficiency. The discharged energy density of neat PEI and the PEI/HfO_2 nanocomposites are summarized in Fig. S1b. The data indicated that the 3 vol% HfO_2-filled PEI nanocomposite can reach a breakdown field near 600 MV/m with maximum discharged energy density of 5.71 J/cm^3 and efficiency of 77.5%. At above 95% efficiency, the discharged energy density of the 3 vol% HfO_2-filled PEI nanocomposite is 3.45 J/cm^3, which far exceeds that of BOPP (~2 J/cm^3) [1,4].

Electrical conduction is known to play a dominant role in determining the insulation strength of dielectrics at high applied fields [13,41,42]. The leakage current density of neat PEI and the PEI/HfO_2 nanocomposites at an electric field of 100 MV/m was measured and shown in Fig. 3b. Owing to the wide bandgap (~5.8 eV) nature of the incorporated HfO_2 fillers, the leakage current density of the PEI/HfO_2 nanocomposites decreases substantially in comparison to that of neat PEI. The lowest leakage current density value is achieved in the 3 vol% HfO_2-filled PEI nanocomposite, which accounts for its highest breakdown strength and the best discharged energy density among the composites. With the further increase of the HfO_2 content, the leakage current density of the composites increases, thus

decreasing the charge–discharge efficiency and discharge energy density (Fig. 3b) [43]. This is possibly owing to the fact that the nanofillers act as shallow traps at high filler contents to increase the carrier mobility of the nanocomposites. Moreover, the distance between the nanoparticles decreases with increase of the HfO_2 contents, which facilitates the formation of conduction path to increase the leakage current.

To assess the reliability and stability of the PEI/HfO_2 nanocomposites, *D*–*E* loops under three different temperatures are depicted in Fig. S1. The maximum discharged energy density as a function of temperature are established and displayed in Fig. 4, where the maximum discharged energy density of PEI and the PEI/HfO_2 nanocomposites declines consistently with temperature. The maximum discharged energy density of neat PEI is reduced from 3.90 J/cm^3 at 25 °C to 2.46 J/cm^3 and 1.60 J/cm^3 at 100 °C and 150 °C, respectively. The 3 vol% HfO_2-filled PEI nanocomposite delivers the energy densities of 5.71, 3.70 and 2.82 J/cm^3 at 25, 100 and 150 ^{o}C, which are 46.4 %, 50.4 % and 76.3 % higher than those of neat PEI, respectively. For all temperatures investigated, the discharged energy densities of the composites are maximized consistently at 3 vol% HfO_2 (Fig. 4).

To further reveal the effect of temperature on the capacitive performance, the energy storage properties and electrical conduction of the 3 vol% HfO_2-filled PEI nanocomposite in comparison to those of neat PEI at various temperatures are depicted in Fig. 5a-c. Due to the nonlinear increase of electrical conduction with the temperature at high applied fields [41, 44–4647], the energy storage properties deteriorate with the increase of the electric field and temperature. The values of U_t/U_{25} and η_t/η_{25} were used to evaluate the change of the discharged energy density and the charge–discharge efficiency,

respectively, where U_t and η_t are defined as the discharged energy density and the charge–discharge efficiency at various temperatures, respectively. For example, as shown in Fig. S2, at an electric field of 400 MV/m, η_{100}/η_{25} are 83.5% and 93.8% for neat PEI and the 3 vol% HfO_2-filled PEI nanocomposite, respectively. U_{100}/U_{25} is 85.6% and 94.2% for neat PEI and the 3 vol% HfO_2-filled PEI nanocomposite, respectively. Apparently, the incorporation of HfO_2 significantly limits the reduction of the discharged energy density and the charge–discharge efficiency of PEI at elevated temperatures and high fields and thus gives rise to the improved high-temperature capacitive performance of the PEI/HfO_2 nanocomposites.

The enhancement in high-temperature capacitive performance of the PEI/HfO_2 nanocomposites is due to the suppressed leakage current arising from the incorporated HfO_2 nanofillers. The leakage current density of neat PEI and the 3 vol% HfO_2-filled PEI nanocomposite at various temperatures are shown in Fig. 5c. While the leakage current density increases with temperature, the leakage current density of the 3 vol% HfO_2-filled PEI nanocomposite is consistently lower than that of neat PEI. The enhancement/reduction ratio of the nanocomposite relative to neat polymer is defined as $R_x=|X_{com}-X_{neat}|/X_{neat}*100\%$, where X can be the discharged energy density (U) or leakage current density (J), subscript 'com' and 'neat' represent the nanocomposite and neat polymer, respectively. As shown in Fig. 5d, the reduction ratios of leakage current density R_J are 8.7%, 40.1% and 70.7% at 25, 100 and 150 ^oC, respectively. Concurrently, the enhancement ratios of the discharged energy density R_U increase from 46.4% at 25 ^oC to 50.4 % and 76.3 % at 100 and 150 ^oC, respectively. Apparently, the positive impact of HfO_2 on the reduction of

electrical conduction and the increase of discharged energy density becomes more significant with increasing temperature.

The comparison of the charge-discharge behavior of neat PEI and the PEI/HfO_2 composites at different temperatures is given in Fig.S4. Apparently, the PEI/HfO2 composite not only delivers higher power densities at varied temperature, *e.g.* 0.22 MW/cm^3 *vs.* 0.18 MW/cm^3 of PEI at 150 ^{o}C, but also presents much higher stability in discharge time, e.g. varying from 2.41- 2.40 μs *vs.* 2.43-2.65 μs of PEI with increasing temperature from 25 to 150 ^{o}C. Therefore, the incorporation of HfO_2 introduces comprehensive improvements in high-temperature capacitive performance, including higher discharge energy density, faster discharge speed, greater power density and better stability at elevated temperatures.

4. Discussion

The high-temperature capacitive energy storage performance of neat PEI and the PEI/HfO_2 nanocomposite has been compared with commercially available high-temperature dielectric polymers, including PC, fluorene polyester (FPE), Kapton® PI and PEEK. As shown in Fig. S3, the PEI/HfO_2 nanocomposite exhibits the best performance at 150 ^{o}C. For example, at an electric field of 250 MV/m, the PEI/HfO_2 nanocomposite delivers a discharged energy density of 0.94 J/cm^3 along with an efficiency of 92.1%, while the discharged energy densities of the high-temperature polymers are below 0.85 J/cm^3 with efficiencies less than 80%. Further increase in the applied field results in the failure of the high-temperature polymers, but the PEI/HfO_2 nanocomposite can operate up to 500 MV/m with an impressive discharged energy density of 2.82 J/cm^3. Fig. 6a compares the

maximum discharged energy density and the corresponding charge–discharge efficiency of PEI/HfO_2 nanocomposite with the current high-temperature dielectric polymers at 150 °C. The maximum discharged energy densities are 1.67, 1.19, 0.53 and 0.53 J/cm^3 for PC, FPE, Kapton® PI and PEEK, respectively. Notably, the nanocomposite consisting of PEI/HfO_2 delivers the maximum discharged energy density of 2.82 J/cm^3, which distinctly outperforms the current high-temperature dielectric polymers. The leakage current densities of the high-temperature polymers and the PEI/HfO_2 nanocomposite are shown in Fig. 6b. The lowest leakage current density found in PEI is responsible for its best high-temperature capacitive performance among the high-temperature neat polymers. The introduction of HfO_2 into PEI further reduces the leakage current density of the resultant composite.

To rationalize the superior energy storage performance of the composites at elevated temperatures, the interface structure and electrical conduction of the PEI/HfO_2 nanocomposite is discussed. According to the multi-core model proposed by Tanaka [48], the interface area consists of a bonding layer, a bound layer and a loose layer which are overlapped by the Gouy-Chapman diffuse layer [49]. When the electric field is applied, carriers in the nanocomposite establish a Gouy-Chapman diffuse layer and generate traps to affect the dielectric properties of the nanocomposite. Based on multi-core models, the interface can act as traps that have significant trapping and scattering effects on carriers. It has been proposed that the high-temperature energy storage properties of the polymer nanocomposites are dominated by the band structure of the fillers [35]. The band diagrams at the polymer/nanofiller interface of the PEI/HfO_2 nanocomposite are depicted in Fig. 7a. Estimated from first-principles calculations, the bandgap and the electron affinity of PEI are 3.2 eV and 2.2 eV, respectively [32]. The bandgap and the electron affinity of HfO_2 are

5.8 eV and 2.5 eV, respectively [35,50]. Owing to a vast difference between the bandgaps, deep traps are created in the interface region which can capture charge carriers and reduce charge density in the polymer composite.

The thermally stimulated depolarization current (TSDC) measurements have been conducted to understand the charge carrier conduction and verify the band diagram analysis at the polymer/nanofiller interface. As shown in Fig.S5, the peak at lower temperature corresponds to relaxation of dipoles such as carbonyl (C=O) groups, while the peak at higher temperature is related to de-trapping of trapped charges. The increase of peak temperature and intensity in the PEI/HfO_2 nanocomposites relative to those of neat PEI implies that more traps with deeper trap depth are formed in the nanocomposites. These traps can impede charge carrier transport and lower conduction current density in the nanocomposites.

The electrical conduction processes, including charge injection from the electrode, charge transport, and charge trapping and de-trapping, in neat PEI and the PEI/HfO_2 nanocomposite are illustrated in Fig. 7b and 7c, respectively. At low fields and low temperatures, the charge density participating conduction processes in the polymer and composites are limited by injection due to lack of thermal or electrical stimulation. In this case, the conduction current in the polymer and composite are both low and the conduction suppression effect brought by inclusion of HfO_2 nanoparticles is limited. At high fields and elevated temperatures, more charges gain sufficient energies to overcome the potential barrier and be injected into the bulk, which results in a significant increase in conduction current of neat PEI. Different from neat PEI, the hole traps at the interface of polymer matrix and nanofiller that introduced by the inclusive of HfO_2 nanoparticles gives full play

to its potential in impeding charge carrier transport in the nanocomposite. As evidenced by the largely reduced leakage current density, the incorporation of the nanofillers with large bandgap impedes electrical conduction, thereby yielding improved discharge energy density and high charge–discharge efficiency at high fields and elevated temperatures.

5. Conclusions

In this work, the PEI nanocomposites filled with HfO_2 nanoparticles have been prepared. Different from the typical nanocomposites in which inorganic fillers with high or low dielectric constants are preferred, HfO_2 nanoparticles with a modest dielectric constant are selected as the fillers. It is found that, owing to a medium dielectric constant and a wide bandgap nature of HfO_2 filler, the nanocomposites exhibit simultaneously enhanced dielectric constant and reduced leakage current density. As a result, remarkable improvements in the electric displacement, discharged energy density and charge–discharge efficiency are concurrently achieved in the HfO_2 filled nanocomposites at elevated temperatures. The 3 vol% HfO_2-filled PEI nanocomposite delivers the maximum discharged energy density of 2.82 J/cm^3 at 150 °C, which outperforms the current high-temperature dielectric polymers. These results provide a new route to improve the high-temperature energy storage properties of dielectric polymer nanocomposites by incorporating nanofillers with medium dielectric constants.

Acknowledgements

L. Ren is grateful for the support from the China Scholarship Council (CSC).

Appendix A. Supplementary data

See supplementary material for energy storage performance of neat PEI and the PEI/HfO_2 nanocomposites at various temperatures, as well as comparison of PEI/HfO_2 nanocomposites and commercial high-temperature polymers as a function of electric field at 150 °C.)

References

[1] H. Li, F. Liu, B. Fan, D. Ai, Z. Peng, Q. Wang, Nanostructured ferroelectric-polymer composites for capacitive energy storage, Small Methods 2(6) (2018) 1700399.

[2] L. Zhu, Exploring strategies for high dielectric constant and low loss polymer dielectrics, J. Phys. Chem. Lett. 5(21) (2014) 3677-3687.

[3] M Rabuffi, G Picci, Status quo and future prospects for metallized polypropylene energy storage capacitors, IEEE Trans. Plasma Sci. 30(5) (2002) 1939-1942.

[4] Z. M. Dang, J. Yuan, J. Zha, T. Zhou, S. Li, G. Hu, Fundamentals, processes and applications of high-permittivity polymer–matrix composites, Prog. Mater. Sci. 57(4) (2012) 60-723.

[5] Y. Zhou, Q. Li, B. Dang, Y. Yang, T. Shao, H. Li, J. Hu, R. Zeng, J. He, Q. Wang, A scalable, high-throughput, and environmentally benign approach to polymer dielectrics exhibiting significantly improved capacitive performance at high temperatures, Adv. Mater. 30(49) (2018) 1805672.

[6] Q. Li, F. Z. Yao, Y. Liu, G. Zhang, H. Wang, Q. Wang, High-temperature dielectric materials for electrical energy storage, Annu. Rev. Mater. Res. 48 (2018) 219-243.

[7] S. Gupta, I. Offenbach, J. Ronzello, Y. Cao, S. Boggs, R. A. Weiss, M. Cakmak, Evaluation of poly(4-methyl-1-pentene) as a dielectric capacitor film for high-temperature energy storage applications, J. Polym. Sci. Part B 55(20) (2017) 1497-1515.

[8] C. Kerwien, D. Malandro, J. Broomall, Large area DC dielectric breakdown voltage measurement of BOPP and PTFE thin films, IEEE Conf. Electl. Insul. Dielectr. Phen. (CEIDP), (2016) 486-489.

[9] J. S. Ho, S. G. Greenbaum, Polymer capacitor dielectrics for high temperature applications, ACS Appl. Mater. Interfaces 10(35) (2018) 29189-29218.

[10] D. Tan, L. Zhang, Q. Chen, P. Irwin, High-temperature capacitor polymer films. J. Electron. Mater. 43(12) (2014) 4569-4575.

[11] J. Pan, K. Li, S. Chuayprakong, T. Hsu, Q. Wang, High-temperature poly (phthalazinone ether ketone) thin films for dielectric energy storage, ACS Appl. Mater. Interfaces 2(5) (2010) 1286-1289.

[12] Y. Zhou, Q. Wang, Advanced polymer dielectrics for high temperature capacitive energy storage, J. Appl. Phys. 127(24) (2020) 240902.

[13] B. Fan, F. Liu, G. Yang, H. Li, G. Zhang, S. Jiang, Q. Wang, Dielectric materials for high-temperature capacitors, IET Nanodielectrics 1(1) (2018) 32-40.

[14] Q. Li, M. Gadinski, S. Zhang, G. Zhang, H. Li, E. Iagodkine, A. Haque, L. Q. Chen, T. Jackson, Q. Wang, Flexible high-temperature dielectric materials from polymer nanocomposites, Nature 523(7562) (2015) 576-579.

[15] H. Li, D. Ai, L. Ren, Z. Han, Z. Shen, J. Wang, L. Q. Chen, Q. Wang, Scalable polymer nanocomposites with record high-temperature capacitive performance enabled by rationally designed nanostructured inorganic fillers, Adv. Mater. 31(23) (2019) 1900875.

[16] H. Li, Z. Xie, L. Liu, Z. Peng, Q. Ding, L. Ren, D. Ai, W. Reainthippayasakul, Y. Huang, Q. Wang, High-performance insulation materials from poly(ether imide)/boron nitride nanosheets with enhanced DC breakdown strength and thermal stability, IEEE Trans. Dielectr. Electr. Insul. 26(3) (2019) 722-729.

[17] J. Bright, Polyetherimide: High temperature, melt processable insulation, IEEE Electr. Insul, Conf. (EIC) (1983) 206-210.

[18] P. Irwin, D. Tan, Y. Cao, N. Silvi, M. Carter, M. Rumler, C. Garet, Development of high temperature capacitors for high density, high temperature applications, SAE Int. J. Aerosp. 1(1) (2008) 817-821.

[19] H. Li, L. Ren, D. Ai, Z. Han, Y. Liu, B. Yao, Q. Wang, Ternary polymer nanocomposites with concurrently enhanced dielectric constant and breakdown strength for high-temperature electrostatic capacitors, InfoMat 2(2) (2020) 389-400.

[20] Z. Li, F. Liu, G. Yang, H. Li, L. Dong, C. Xiong, Q. Wang, Enhanced energy storage performance of ferroelectric polymer nanocomposites at relatively low electric fields induced by surface modified $BaTiO_3$ nanofibers, Compos. Sci. Technol. 164 (2018) 214-221.

[21] Y. Wang, L. Wang, Q. Yuan, J. Chen, Y. Niu, X. Xu, Y. Cheng, B. Yao, Q. Wang, H. Wang, Ultrahigh energy density and greatly enhanced discharged efficiency of sandwich-structured polymer nanocomposites with optimized spatial organization, Nano Energy 44 (2018) 364-370.

[22] Y. Zhu, P. Jiang, X. Huang, Poly(vinylidene fluoride) terpolymer and poly(methyl methacrylate) composite films with superior energy storage performance for electrostatic capacitor application, Compos. Sci. Technol. 179 (2019) 115-124.

[23] Q. Chi, Z. Gao, T. Zhang, C. Zhang, Y. Zhang, Q. Chen, X. Wang, Q. Lei, Excellent energy storage properties with high-temperature stability in sandwich-structured polyimide-based composite films, ACS Sustainable Chem. Eng. 7(1) (2018) 748-757.

[24] H. Bai, G. Ge, X. He, B. Shen, J. Zhai, H. Pan, Ultrahigh breakdown strength and energy density of polymer nanocomposite containing surface insulated BCZT@ BN nanofibers, Compos. Sci. Technol. (2020) 108209.

[25] D. He, Y. Wang, S. Song, S. Liu, Y. Luo, Y. Deng, Polymer-based nanocomposites employing Bi_2S_3@ SiO_2 nanorods for high dielectric performance: understanding the role of interfacial polarization in semiconductor-insulator core-shell nanostructure, Compos. Sci. Technol. 151 (2017). 25-33

[26] X. Zhang, J. Jiang, Z. Shen, Z. Dan, M. Li, Y. Lin, C. W. Nan, L. Q. Chen, Y. Shen, Polymer nanocomposites with ultrahigh energy density and high discharge efficiency by modulating their nanostructures in three dimensions, Adv. Mater. 30(16) (2018) 1707269.

[27] X. Liang, X. Yu, L. Lv, T. Zhao, S. Luo, S. Yu, R. Sun, C. P. Wong, P. Zhu, $BaTiO_3$ internally decorated hollow porous carbon hybrids as fillers enhancing dielectric and energy storage performance of sandwich-structured polymer composite, Nano Energy 68 (2020) 104351.

[28] S. Luo, Y. Shen, S. Yu, Y. Wan, W. H. Liao, R. Sun, C. P. Wong, Construction of a 3D-$BaTiO_3$ network leading to significantly enhanced dielectric permittivity and energy storage density of polymer composites, Energy Environ. Sci. 10(1) (2017) 137-144.

[29] Y. Wang, J. Chen, Y. Li, Y. Niu, Q. Wang, W. Hong, Multilayered hierarchical polymer composites for high energy density capacitors, J. Mater. Chem. A 7(7) (2019) 2965-2980.

[30] Y. Dang, M. Zheng, J. Zha, Improvements of dielectric properties and energy storage performances in $BaTiO_3$/PVDF nanocomposites by employing a thermal treatment process, J. Adv. Dielectr. 8(6) (2018) 1850043.

[31] H. Li, L. Ren, Y. Zhou, B. Yao, Q. Wang, Recent progress in polymer dielectrics containing boron nitride nanosheets for high energy density capacitors, High Volt. (2020)

[32] A. Azizi, M. Gadnski, Q. Li, M. Alsaud, J. Wang, Y. Wang, B. Wang, F. Liu, L.Q. Chen, N. Alem, Q. Wang, High-performance polymers sandwiched with chemical vapor deposited hexagonal boron nitrides as scalable high-temperature dielectric materials, Adv. Mater. 29(35) (2017) 1701864.

[33] G. Liu, T. Zhang, Y. Feng, Y. Zhang, C. Zhang, Y. Zhang, X. Wang, Q. Chi, Q. Chen, Q. Lei, Sandwich-structured polymers with electrospun boron nitrides layers as high-temperature energy storage dielectrics, Chem. Eng. J. 389 (2020) 124443.

[34] Y. Zhu, Y. Zhu, X. Huang, J. Chen, Q. Li, J. He, P. Jiang, High energy density polymer dielectrics interlayered by assembled boron nitride nanosheets, Adv. Energy Mater. 9 (2019) 1901826.

[35] D. Ai, H. Li, Y. Zhou, L. Ren, Z. Han, B. Yao, W. Zhou, L. Zhao, J. Xu, Q. Wang, Tuning nanofillers in in situ prepared polyimide nanocomposites for high-temperature capacitive energy storage, Adv. Energy Mater. 10(16) (2020) 1903881.

[36] C. Chen, Y. Xie, J. Liu, J. Li, X. Wei, Z. Zhang, Enhanced energy storage capability of P(VDF-HFP) nanodielectrics by HfO_2 passivation layer: preparation, performance and simulation, Compos. Sci. Technol. 188 (2020) 107968.

[37] H. Luo, X. Zhou, C. Ellingford, Y. Zhang, S. Chen, K. Zhou, D. Zhang, C. R. Bowen, C. Wan, Interface design for high energy density polymer nanocomposites, Chem. Soc. Rev. 48(16) (2019) 4424-4465.

[38] X. Zhang, B. Li, L. Dong, H. Liu, W. Chen, Y. Shen, C. W. Nan, Superior energy storage performances of polymer nanocomposites via modification of filler/polymer interfaces, Adv. Mater. Interfaces 5(11) (2018) 1800096.

[39] S. Chen, Y. Zhou, H. Luo, L. Tang, R. Guo, D. Zhang, Core-shell TiO_2@ HfO_2 nanowire arrays with designable shell thicknesses for improved permittivity and energy density in polymer nanocomposites, Compos. Part A (2020) 106012.

[40] L. Wu, N. Luo, Z. Xie, Y. Liu, F. Chen, Q. Fu, Improved breakdown strength of Poly (vinylidene fluoride)-based composites by using all ball-milled hexagonal boron nitride sheets without centrifugation, Compos. Sci. Technol. 190 (2020) 108046.

[41] J. Ho, T. Jow, High field conduction in biaxially oriented polypropylene at elevated temperature, IEEE Trans. Dielectr. Electr. Insul. 19(3) (2012) 990-995.

[42] G. Zhang, Y. Li, S. D. Tang, R. D. Thompson, L. Zhu, The role of field electron emission in polypropylene/aluminum nanodielectrics under high electric fields, ACS Appl. Mater. Interfaces 9(11) (2017) 10106-10119.

[43] Y. Huang, D. Min, S. Li, X. Wang, S. Lin, Dielectric relaxation and carrier transport in epoxy resin and its microcomposite, IEEE Trans. Dielectr. Electr. Insul. 24(5) (2017) 3083-3091.

[44] Z. Zhang, D. Wang, M. H. Litt, L. S. Tan, L. Zhu, High-temperature and high-energy-density dipolar glass polymers based on sulfonylated poly(2, 6-dimethyl-1, 4-phenylene oxide), Angew. Chem. Int. Ed. 130(6) (2018) 1544-1547.

[45] H. Li, M. R. Gadinski, Y. Huang, L. Ren, Y. Zhou, D. Ai, Z. Han, B. Yao, Q. Wang, Crosslinked fluoropolymers exhibiting superior high-temperature energy density and charge–discharge efficiency, Energy Environ. Sci. 13(4) (2020) 1279-1286.

[46] Y. Thakur, M. H. Lean, Q. M. Zhang, Reducing conduction losses in high energy density polymer using nanocomposites, Appl. Phys. Lett. 110(12) (2017) 122905.

[47] J. Chen, Y. Wang, Q. Yuan, X. Xu,Y. Niu, Q. Wang, H. Wang, Multilayered ferroelectric polymer films incorporating low-dielectric-constant components for concurrent enhancement of energy density and charge–discharge efficiency, Nano Energy 54 (2018) 288-296.

[48] T. Tanaka, M. Kozako, N. Fuse, Y. Ohki, Proposal of a multi-core model for polymer nanocomposite dielectrics, IEEE Trans. Dielectr. Electr. Insul. 12(4) (2005) 669-681.

[49] V. K. Thakur, R. K. Gupta, Recent progress on ferroelectric polymer-based nanocomposites for high energy density capacitors: synthesis, dielectric properties, and future aspects, Chem. Rev. 116(7) (2016) 4260-4317.

[50] J. Robertson, Band offsets of wide-band-gap oxides and implications for future electronic devices, J. Vac. Sci. Technol. B 18(3) (2000) 1785-1791.

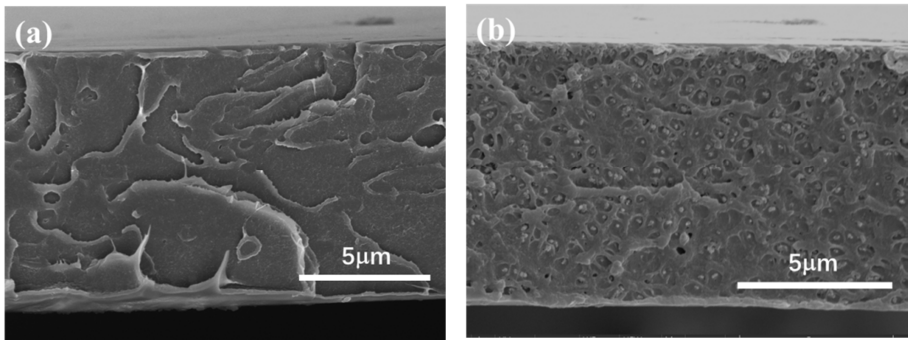

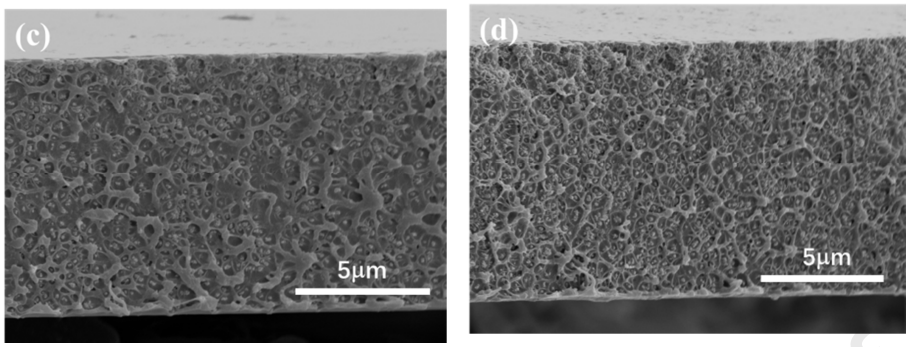

Fig. 1. Cross-sectional SEM images of (a) neat PEI and the PEI/HfO_2 nanocomposites with filler contents of (b) 1 vol% (c) 5 vol% and (d) 9 vol%.

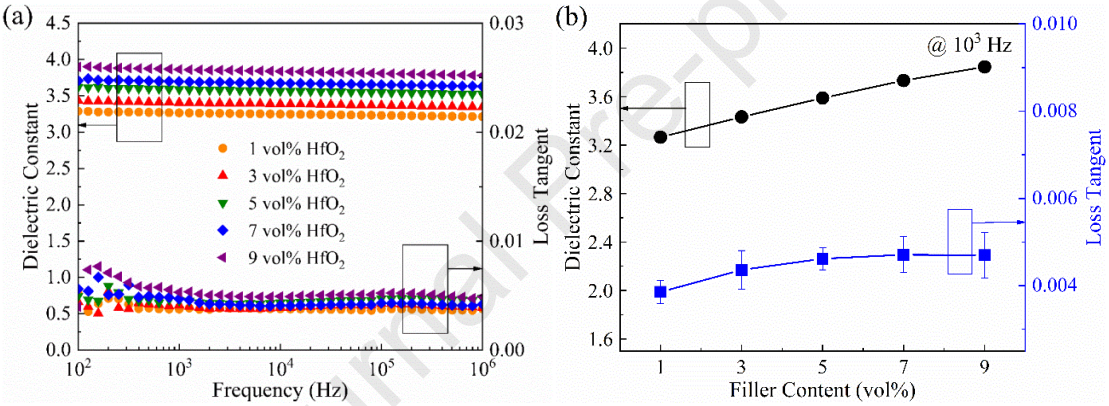

Fig. 2. (a) Dielectric spectra of the PEI/HfO_2 nanocomposites with varied filler contents. (b) Dielectric constant and loss tangent of the PEI/HfO_2 nanocomposites as a function of filler content.

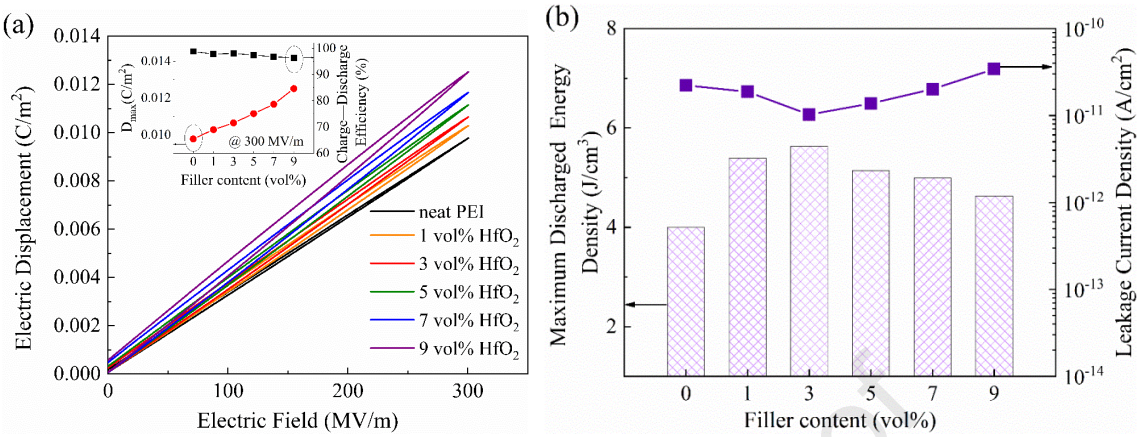

Fig. 3. (a) Electric displacement–electric field (*D*–*E*) loops of neat PEI and the PEI/HfO_2 nanocomposites at 300 MV/m (Inset: Displacement and charge–discharge efficiency of neat PEI and the PEI/HfO_2 nanocomposites at 300 MV/m as a function of filler content) (b) Maximum discharged energy density and leakage current density of neat PEI and the PEI/HfO_2 nanocomposites as a function of filler content.

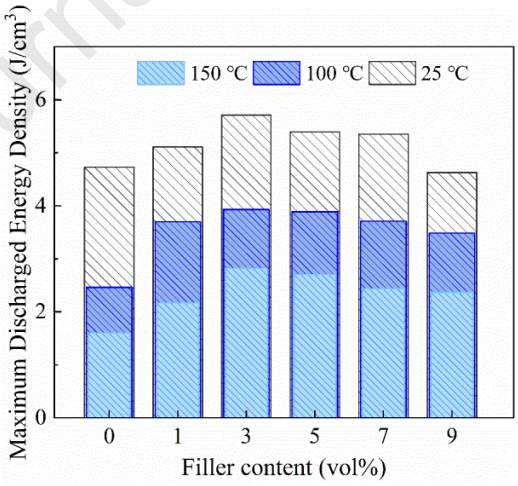

Fig. 4. Maximum discharged energy density of neat PEI and the PEI/HfO_2 nanocomposites as a function of the filler content at various temperatures.

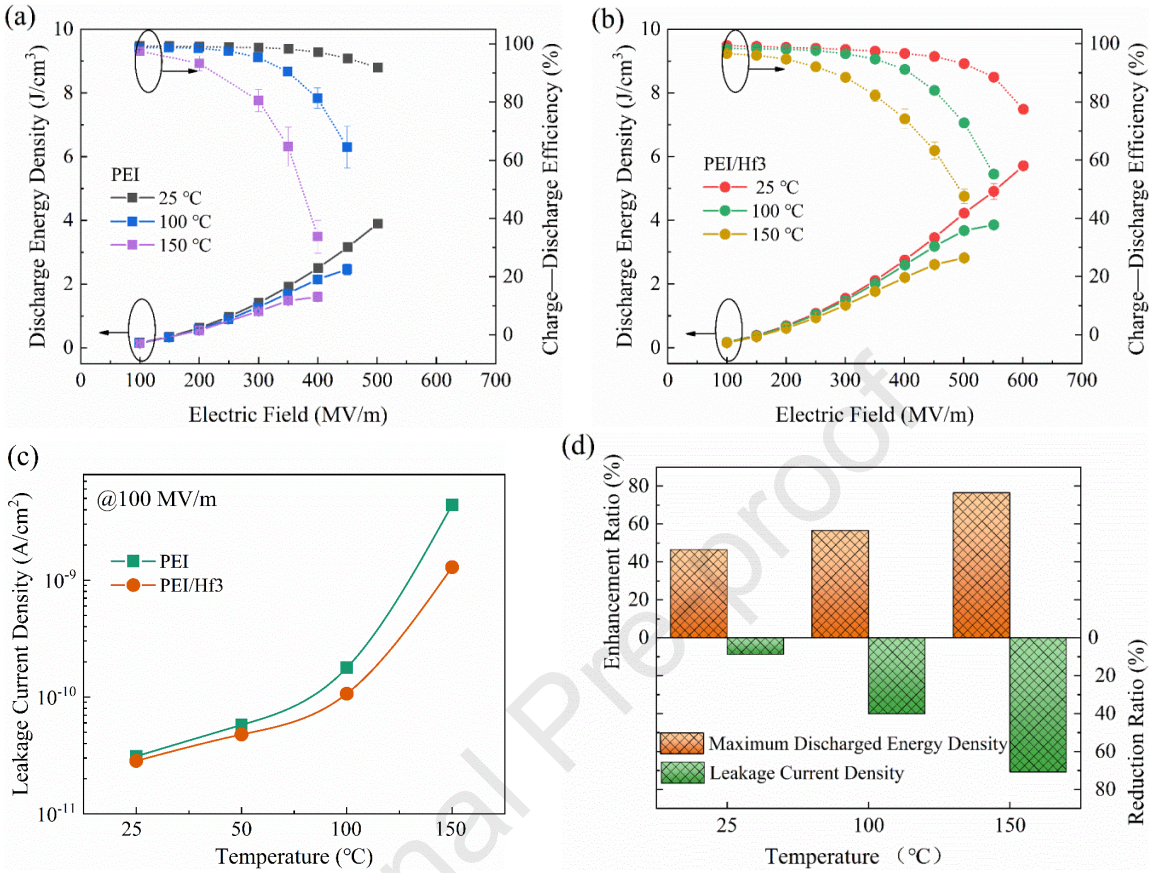

Fig. 5. Discharged energy density and charge–discharge efficiency at various temperatures of (a) neat PEI and (b) the 3 vol% HfO_2-filled PEI nanocomposite. (c) Leakage current density of neat PEI and the 3 vol% HfO_2-filled PEI nanocomposite at various temperatures. (d) Reduction/enhancement ratio of maximum discharged energy density and leakage current density of the 3 vol% HfO_2-filled PEI nanocomposite at various temperatures.

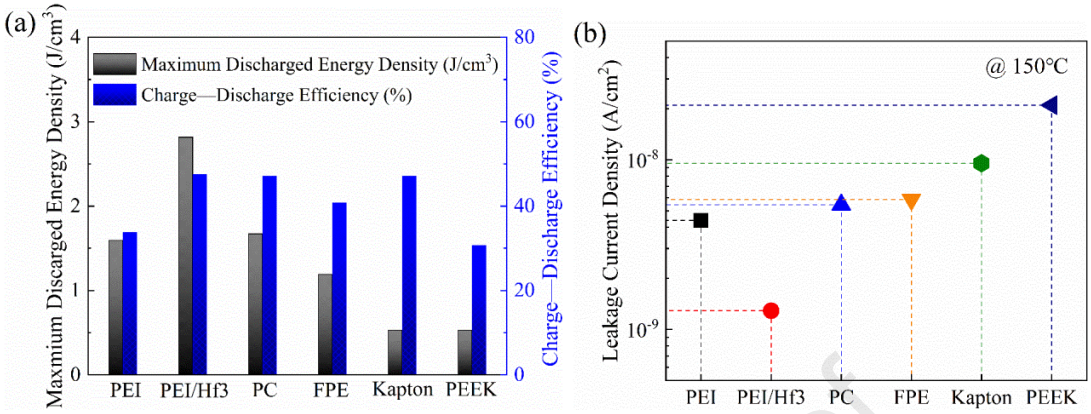

Fig. 6. (a) Maximum discharged energy density and the corresponding charge–discharge efficiency (b) Leakage current density at 100 MV/m of neat PEI, the 3 vol% HfO_2-filled PEI nanocomposite, PC, FPE, Kapton® PI and PEEK at 150 °C.

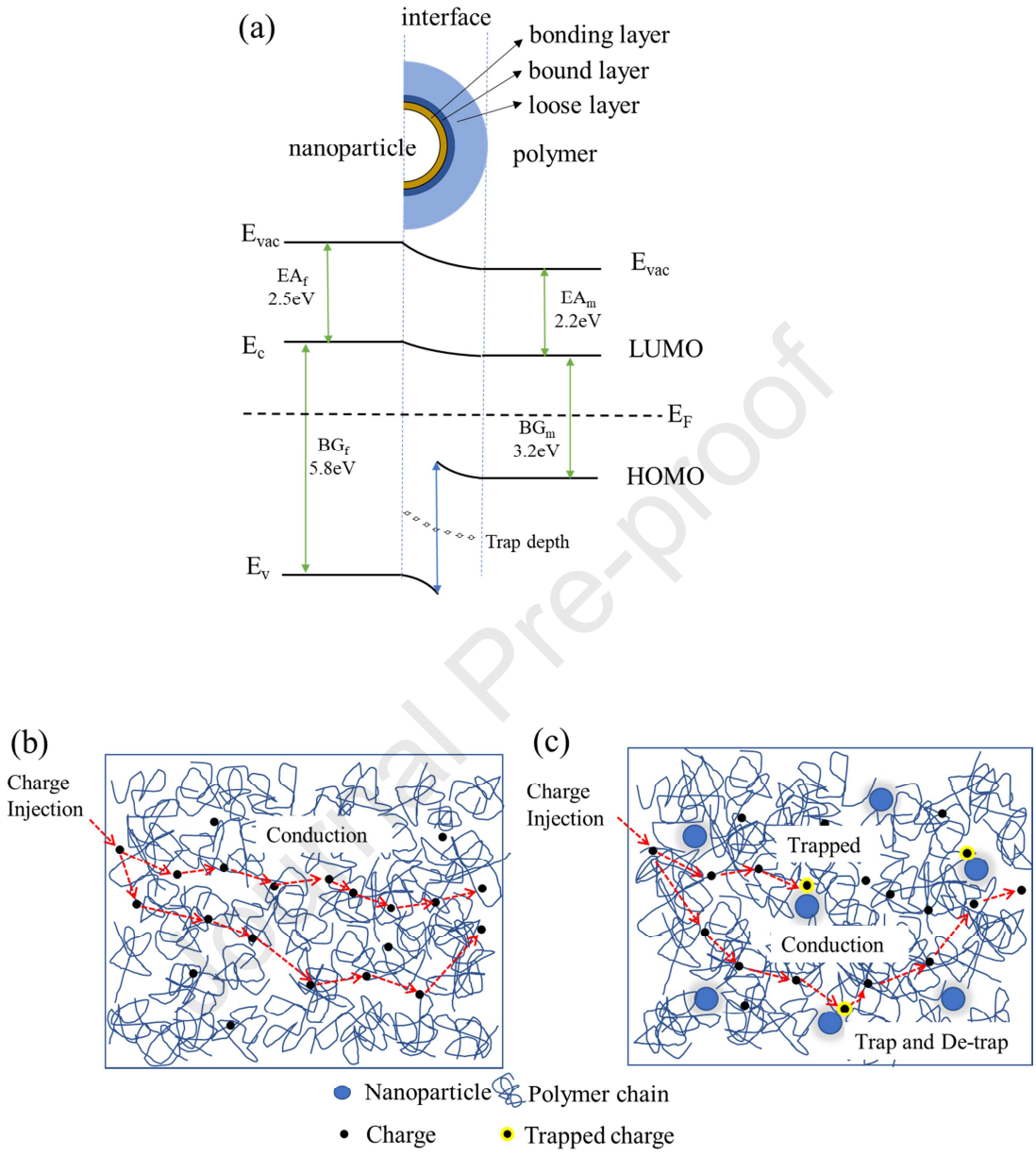

Fig. 7. (a) Band diagrams at the polymer/nanofiller interface. E_{vac} is the vacuum energy level, E_f is the Feimi energy level. E_c, E_v, EA_f, BG_f are the conduction band, valence band, electron affinity and bandgap of the nanofiller, respectively. LUMO, HOMO, EA_m, BG_m are the lowest unoccupied molecular orbital, highest occupied molecular orbital, electron

affinity and bandgap of the polymer matrix, respectively. Schematic of conduction processes in (b) neat PEI and (c) the PEI/HfO_2 nanocomposite.

The authors declare no competing financial interests.